Structure of mouse 7S NGF: a complex of nerve growth factor with four binding proteins

Ben Bax[1]*, Tom L Blundell[1†], Judith Murray-Rust[1,2] and Neil Q McDonald[1,2]

Background: Nerve growth factor (NGF) is a neurotrophic factor that promotes the differentiation and survival of certain populations of neurons in the central and peripheral nervous systems. 7S NGF is an $\alpha_2\beta_2\gamma_2$ complex in which the β-NGF dimer (the active neurotrophin) is associated with two α-NGF and two γ-NGF subunits, which belong to the glandular kallikrein family of serine proteinases. The γ-NGF subunit is an active serine proteinase capable of processing the precursor form of β-NGF, whereas α-NGF is an inactive serine proteinase. The structure of 7S NGF could be used as a starting point to design inhibitors that prevent NGF binding to its receptors, as a potential treatment of neurodegenerative diseases.

Results: The crystal structure of 7S NGF shows that the two γ-NGF subunits make extensive interactions with each other around the twofold axis of the complex and have the C-terminal residues of the β-NGF subunits bound within their active sites. The 'activation domain' of each of the α-NGF subunits is in an inactive (zymogen-like) conformation and makes extensive interactions with the β-NGF dimer. The two zinc ions that stabilize the complex are located at the relatively small interfaces between the α-NGF and γ-NGF subunits.

Conclusions: The structure of 7S NGF shows how the twofold axis of the central β-NGF dimer organizes the symmetry of this multisubunit growth factor complex. The extensive surface of β-NGF buried within the 7S complex explains the lack of neurotrophic activity observed for 7S NGF. The regions of the β-NGF dimer that contact the α-NGF subunits overlap with those known to engage NGF receptors. Two disulphide-linked loops on α-NGF make multiple interactions with β-NGF and suggest that it might be possible to design peptides that inhibit the binding of β-NGF to its receptors.

Addresses: [1]ICRF Unit of Structural Molecular Biology, Department of Crystallography, Birkbeck College, Malet Street, London WC1E 7HX, UK and [2]ICRF, 44 Lincolns Inn Fields, London WC2A 3PX, UK.

[†]Present address: Department of Biochemistry, University of Cambridge, Tennis Court Road, Cambridge CB2 1QW, UK.

*Corresponding author.
E-mail: b.bax@cryst.bbk.ac.uk

Key words: kallikrein, nerve growth factor (NGF), protein–protein interactions, serine proteinase

Received: **2 July 1997**
Revisions requested: **31 July 1997**
Revisions received: **18 August 1997**
Accepted: **19 August 1997**

Structure 15 October 1997, **5**:1275–1285
http://biomednet.com/elecref/0969212600501275

Introduction

Nerve growth factor (NGF) is a non-covalently linked dimer consisting of two 118-residue polypeptides, each of which contains three intramolecular disulphide bridges [1]. NGF is a prototypical member of the neurotrophin family of growth factors that promote the differentiation and survival of distinct populations of neurons in both the central and the peripheral nervous systems [2]. Two types of cell-surface receptors are engaged by the neurotrophins for signalling — those belonging to the trk receptor tyrosine kinase family, necessary to maintain neuronal survival, and the p75NTR (p75 neurotrophin receptor), which may initiate quite different intracellular signalling cascades from trk [3]. The structure of NGF [4], a rather elongated dimer containing a cystine-knot motif [5], provided a structural framework for studies of ligand–receptor contacts using mutant, chimeric and chemically modified neurotrophins [6]. These studies indicated that several charged residues within three β-hairpin loops of each neurotrophin are critical for the neurotrophin–p75NTR interaction, whereas a more extended surface is important for neurotrophin–trk receptor interaction [7].

Pioneering studies on the trophic activity of NGF led to the discovery that the male mouse submandibular salivary gland is a rich source of nerve growth factor (reviewed in [8]). In this tissue, NGF exists in a high molecular weight complex (Mr ~140,000) known as 7S NGF due to its sedimentation coefficient [9]. The complex can be dissociated at pH extremes into three components [10] — the active neurotrophic factor β-NGF (also known as NGF) and two related serine proteinases α-NGF and γ-NGF. Binary complexes of a β-NGF dimer with two α-NGF subunits or two γ-NGF subunits can be formed [11]. Although α and γ subunits do not form a demonstrable complex, they apparently interact in 7S NGF to render it more stable than the sum of the α–β and β–γ interactions [11]. The presence of zinc further enhances the stability of the complex and prevents dissociation of γ subunit from 7S NGF [12], but zinc does not stabilize the interaction of γ subunit with β-NGF in the absence of α subunits [13]. Chelation of the zinc by EDTA allows 7S NGF to be readily dissociated by salt at neutral pH [14–16]. While part of the 7S NGF complex, β-NGF is inhibited from binding to receptors on embryonic chick

Table 1

Percentage sequence identity between α-NGF, γ-NGF and other serine proteinases (%)*.

	α-NGF	Tonin†	PPK‡
γ-NGF	78.9	64.3	61.6
α-NGF	100	60.8	56.5
Tonin		100	53.0

*Calculated as the number of identical residues, between residues 16 and 246, divided by the length of the shortest sequence. †Rat tonin; ‡porcine pancreatic kallikrein.

sensory neurons [17,18]. In addition, α-NGF and γ-NGF were both found to block competitively all steady-state binding of β-NGF to PC12 cells [19].

The amino acid sequences of γ-NGF [20,21] and α-NGF [22] showed that they are closely related members of the glandular kallikrein family of serine proteinases (Table 1). Despite the similarity of sequence, α-NGF and γ-NGF have distinct properties — γ-NGF is an active serine proteinase capable of processing the β-NGF precursor protein *in vitro* [23,24], whereas α-NGF is an inactive serine proteinase [25]. The N-terminal sequence of α-NGF is unusual in lacking a basic residue at position 15, conserved among serine proteases, after which cleavage usually takes place to remove the N-terminal zymogen peptide; the N-terminal residue of α-NGF is Ala9 [26].

The first crystal structure solved for a member of the glandular kallikrein family was that of porcine pancreatic kallikrein (PPK) [27,28]. Although the structure of PPK was very similar to that of trypsin, several of the loops around the active site were more prominent in PPK than in trypsin, accounting for the strongly reduced activity of kallikrein towards large protein substrates [27]. The crystal structures of PPK and another glandular kallikrein, rat tonin [29], have been used to model the structures of the α-NGF and γ-NGF subunits, but the structure of the 7S complex could not be predicted [30].

We have previously described the crystallization of 7S NGF [31]. Here, we present the structure of the orthorhombic crystal form of mouse 7S NGF at 3.15 Å resolution. The structure was solved by molecular replacement using the structures of β-NGF [4] and PPK [27] as search molecules. PPK was used as a search model for the α and γ subunits as the structure of tonin is slightly perturbed by a zinc ion from the crystallization buffer that binds at the active site [29].

In the crystal structure we have determined, there is one 7S NGF complex in the asymmetric unit (i.e. two α-NGF subunits — referred to in this paper as subunits α1 and α2, two β-NGF subunits — β1 and β2, and two γ-NGF subunits — γ1 and γ2). In this paper, residues in the α subunits are prefixed with a letter A (e.g. CysA191), residues in the β subunits are prefixed with the letter B and in the γ subunits with the letter G. The residue numbers for the β-NGF subunits refer to full length β-NGF (B1–B118 for subunit β1). The residue nomenclature of the α-NGF and γ-NGF subunits is based on the alignment of the sequences with chymotrypsinogen (e.g. residues belonging to the γ1 subunit are numbered G16–G246). For the α2, β2 and γ2 subunits, 500 has been added to the residue number to distinguish these residues from those in the α1, β1 and γ1 subunits; thus CysA691 in the α2 subunit is equivalent to residue CysA191 in the α1 subunit.

Results and discussion

Structure determination and refinement

The orthorhombic crystal form of 7S NGF (space group $P2_12_12_1$; a = 95.68, b = 96.59, c = 147.00 Å) has one 7S complex in the asymmetric unit with an internal twofold axis some 18.5° away from the b axis (Figure 1; see Materials and methods for details of the structure determination and refinement). The orientations and positions of the β-NGF dimer and the four kallikrein subunits (two α-NGF and two γ-NGF subunits) were determined by molecular replacement making use of the noncrystallographic twofold axis. In the early rounds of refinement, electron-density maps were averaged with

Figure 1

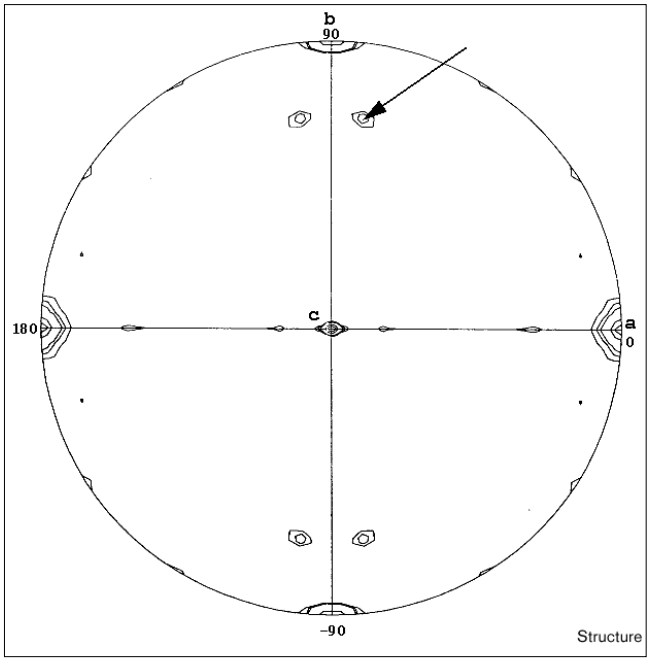

Self-rotation function for 7S NGF. The χ = 180° section of the self-rotation function with the position of the non-crystallographic twofold axis, at ω = 72.5°, φ = 82°, indicated by an arrow (symmetry-related peaks are at ω = 72.5°, φ = 98°; ω = 72.5°, φ = −82°; and ω = 72.5°, φ = −98°).

the RAVE suite of programs [32] and some noncrystallographic symmetry (NCS) constraints/restraints were applied in X-PLOR [33]. The final R-factor and R_{free} after nine rounds of refinement were 24.6 and 28.2%, respectively; inclusion of all data for a final round of positional and group temperature factor refinement lowered the R factor to 24.3% for all data between 8.0–3.15 Å resolution.

Overall structure of 7S NGF

The β-NGF dimer is at the core of the 7S NGF complex surrounded by a horseshoe-like array of α-NGF and γ-NGF subunits (Figure 2). The two α-NGF subunits bind on opposite sides of the β-NGF dimer, whereas the two γ-NGF subunits interact with each other around the twofold axis of the 7S NGF complex, below the β-NGF dimer (Figure 2). The C-terminal residue of each β-NGF subunit (B118 and B618) is bound in the active site of a γ-NGF subunit; these termini probably result from cleavage of the β-NGF precursor by γ-NGF. Two zinc ions, which enhance the stability of the 7S NGF complex, are located at the interface between the α1 and γ1 subunits (and at the equivalent α2–γ2 interface). We describe below the structures of the individual subunits and then the γ–β, α–β, α–γ and γ–γ intersubunit interfaces. Unless stated residues in the second subunits (α2, β2 and γ2) have similar conformations and interactions to the twofold related residues in the first subunits (α1, β1 and γ1).

The C terminus of β-NGF is ordered within 7S NGF

The structure of the β-NGF dimer in the 7S NGF complex (Figure 3) is very similar to that seen in the crystal structures of the isolated β-NGF dimer [4,34], although there are some notable differences particularly at the C terminus. The β-NGF dimer used to solve the 7S structure was that described by McDonald *et al.* [4], lacking residues 1–10 from the N-terminus and residues 112–118 from the C terminus.

Figure 2

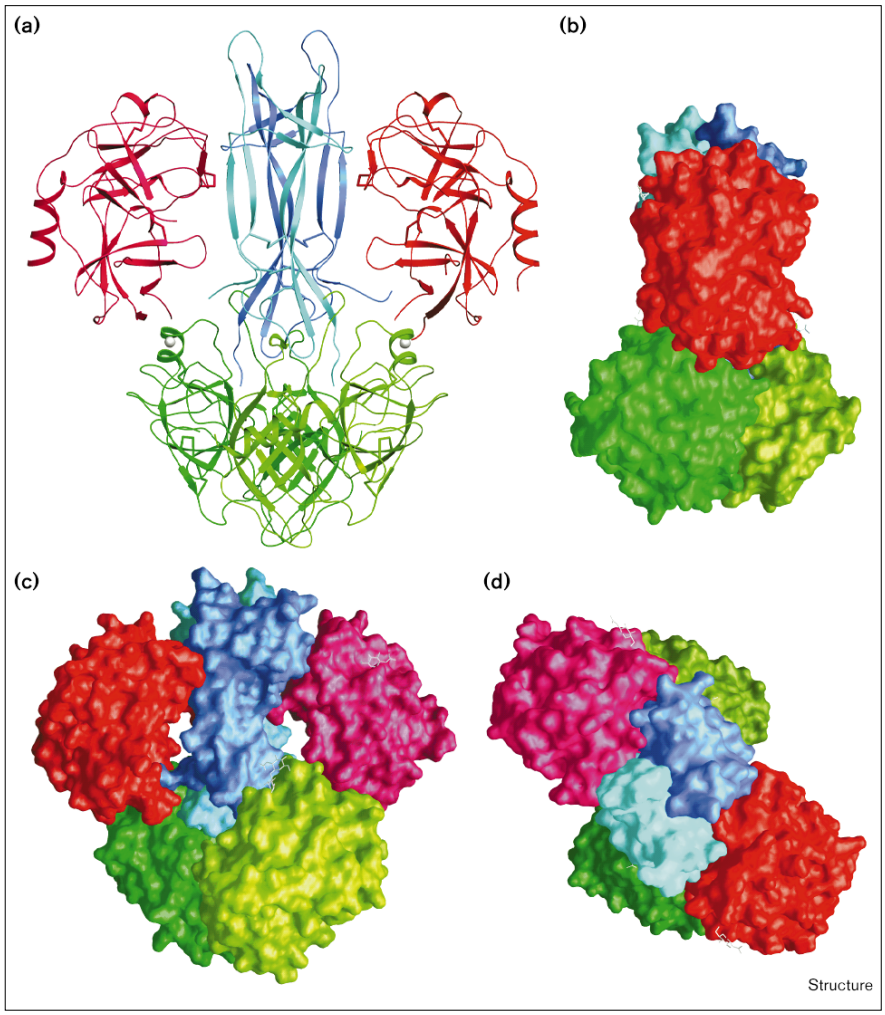

Overall structure of 7S NGF **(a)** Cartoon and **(b–d)** GRASP representations of the interactions among NGF subunits. The β-NGF dimer (β1 subunit light blue and β2 darker blue) is at the centre with the α subunits in red and the γ subunits in green. Interactions between the γ1 and α1 (and γ2 and α2) subunits are mediated by a zinc ion (off-white spheres). Figure 2a was drawn with SETOR [56], and b, c and d with GRASP [57].

Figure 3

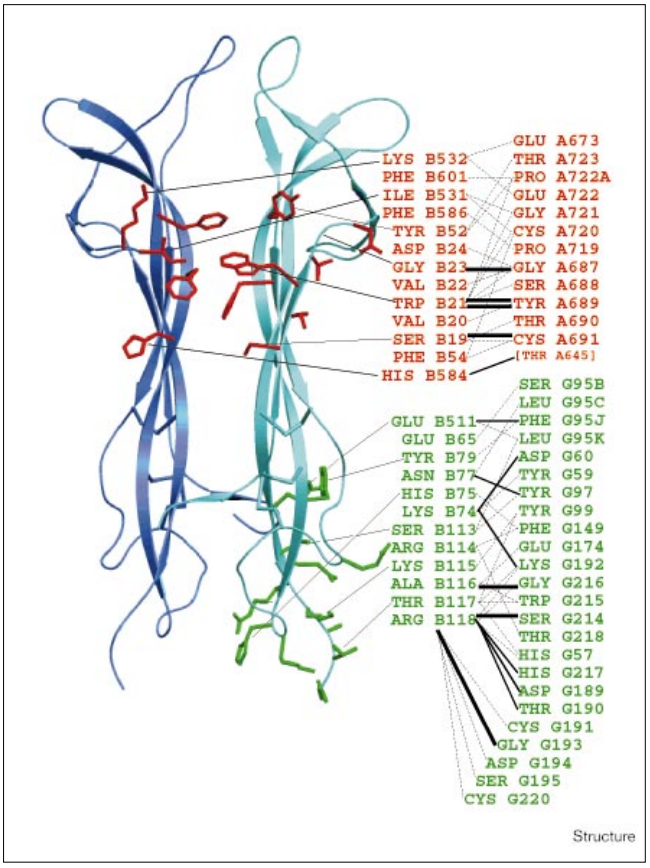

The β-NGF dimer is shown as it appears in the 7S NGF complex, with subunit β1 in light blue and subunit β2 in dark blue, β strands are drawn as arrows. The sidechains of residues that interact with the α2, α-NGF, subunit are shown in red and the sidechains of residues involved in interactions with the γ1, γ-NGF, subunit are in green. Details of residue–residue interactions between the β-NGF dimer and the α2 subunit (red letters), and between the β-NGF dimer and the γ1 subunit (green letters) are shown; thick lines represent mainchain–mainchain hydrogen bonds, thin lines indicate other hydrogen bonds and dotted lines represent contacts < 4 Å. ThrA645 is shown in parentheses as the assignment for this residue is uncertain. Figure was drawn with SETOR [56].

In the 7S complex, residues B112–B118 are well-defined. Residues SerB113 and LysB115 make mainchain hydrogen bonds with AsnB77 and HisB75, respectively, to form an antiparallel β structure, and the sidechain of LysB115 is close to the mainchain carbonyl of SerB73. A similar conformation for residues 112–115 is seen in the crystal structure of *bis*-desocta$_{1-8}$–β-NGF ([34]; PDB code 1BTG) and in the refined structure of β-NGF (PDB code 1BET). In 7S NGF, however, the C-terminal residues have much lower temperature factors and residues B116–B118 are also very well-ordered (presumably because of the interaction with γ-NGF). We note that the zinc ion found adjacent to His84 and Asp105 in two different crystal forms of *bis*-desocta$_{1-8}$–β-NGF [34] is not present in our crystals of 7S NGF.

The N-terminal residues of β-NGF in 7S NGF do not have well-defined electron density; the first residue that has good density is GlyB10 as was also found in the crystal structure of β-NGF [4]. We observe poor electron density for residues preceding GlyB10 and we have tentatively modelled two residues, B509 and B508, into this density in the β2 subunit. These two residues come close to loop 8 of the α1 subunit (see below). Although we expect β-NGF isolated from 7S NGF to have an intact N terminus, the proteolytic removal of the eight N-terminal amino acids does not prevent reassociation of β-NGF with the α and γ subunits to form 7S NGF [35]. Another poorly ordered part of β-NGF is the highly mobile loop at residues 43–47 of β-NGF, which has high temperature factors both in NGF [4] and in 7S NGF.

Structure of γ-NGF, a highly specific kallikrein

γ-NGF is an active serine proteinase with an overall structure (Figure 4) that is similar to those of the closely related glandular kallikreins PPK [27,28] and tonin [29]. Bax *et al.* [30] suggested that six prominent loops around the active site of γ-NGF would be critical for β-NGF recognition (loops 1–6; Figure 4); this is confirmed in the structure of 7S NGF, because contacts between γ-NGF and β-NGF arise primarily from residues within five of these loops (2, 3, 4, 5 and 6) with additional contacts made by a less exposed loop (loop 7; Figures 3 and 4). Loop 3, known as the 'kallikrein loop', and loop 5 adopt conformations unique to γ-NGF, whereas the conformations of the four other prominent loops around the active site resemble those of the corresponding loops in PPK and/or tonin.

The characteristically large kallikrein loop of γ-NGF (Figure 5) makes extensive interactions with β-NGF (Figures 3 and 4) which presumably help to stabilize its conformation (much of this loop is disordered in PPK and tonin). Compared with chymotrypsinogen, γ-NGF has an eleven residue insert in this 'kallikrein loop' and, as these 'extra' residues are 'inserted' between residues 95 and 96 of chymotrypsinogen, they are called G95a–G95k (Figure 5). In the mature form of γ-NGF, four residues (G95f–G95i) have been cleaved from the 'kallikrein loop' [20,21], providing a free α-amino group at PheG95j. In 7S NGF, this free α-amino group of PheG95j makes hydrogen bonds with the hydroxyl of TyrB79 and the carboxylate of GluB512 from the β-NGF dimer. On the N-terminal side of the cleavage site, no density is observed for ArgG95e and poor density is seen for MetG95d (note ArgG95e is absent in some forms of γ-NGF [36,37]). Extending from the glycosylation site of γ-NGF (AsnG95; [20]) there is clear density for two *N*-acetyl glucosamine (NAG) residues, as well as weaker density for additional sugar residues that we have not been able to identify definitively.

Residues from loops 1, 4 and 8 of the γ1 subunit make extensive interactions about the twofold axis of the

Figure 4

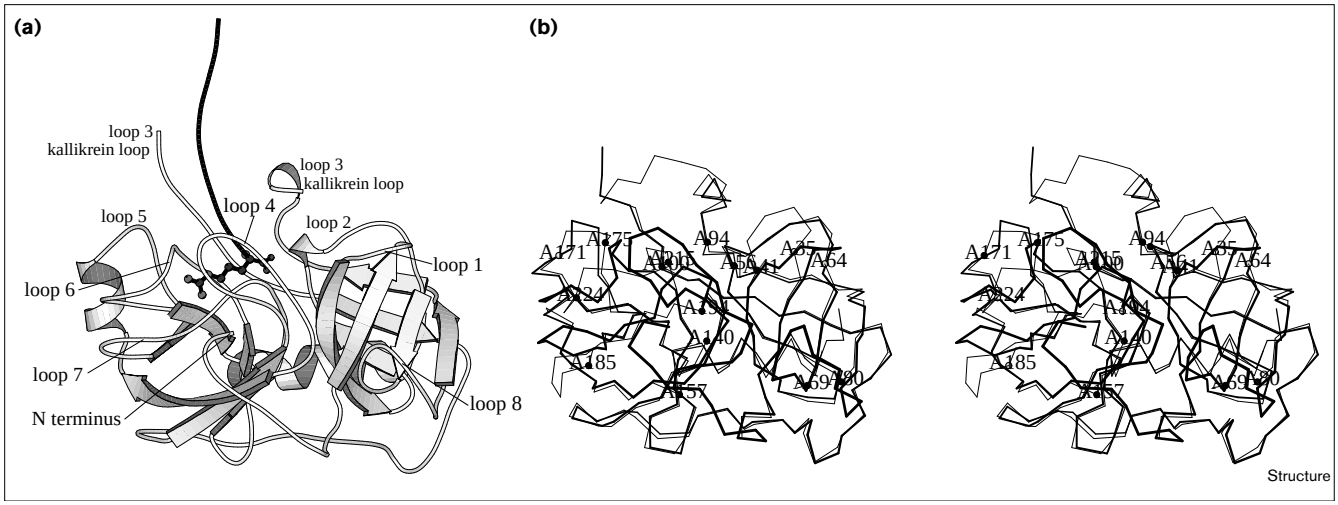

Topology and comparison of the α- and γ-NGF subunits **(a)** Schematic view of the structure of the γ1, γ-NGF, subunit, with the C-terminal arginine of β-NGF in the active-site cleft. Loops discussed in the text are indicated. **(b)** Stereo view (Cα atoms) of the γ1, γ-NGF, subunit and the α2, α-NGF, subunits superposed, the view is the same as in (a). The Cα atoms of α-NGF at the ends of eight loops described in the text are marked with dots and labelled. Figure was drawn with MOLSCRIPT [58].

complex with the corresponding loops in the γ2 subunit. Loop 4 (the 'autolysis loop') contains a second internal site that can be subject to proteolysis (between residues LysG148 and PheG149; [36,37]). Electron density is continuous throughout this loop, however, indicating that no cleavage has occurred in the 7S crystal.

Structure of α-NGF: a 'locked zymogen'

The structure of α-NGF differs substantially from that of γ-NGF at the N terminus and in six loop regions (1, 4, 5, 6, 7 and 8; Figure 4). The difference in conformations of the N terminus and loops 4, 6 and 7 were expected because the unusual sequence of α-NGF (Figure 5) prevents processing from the zymogen precursor to an active enzyme. Activation of a serine proteinase usually occurs by cleavage after a basic residue at position 15, allowing the newly formed amino group of residue 16 to tuck itself into the core and form an ion pair with Asp194; this causes a change in structure of the 'activation domain' (the N terminus and loops 4, 6 and 7; see Figure 4). α-NGF lacks a basic residue at position 15 and, although it was predicted that the structure of α-NGF would be locked into a zymogen-like state [30], it was not clear what conformation the activation domain (residues 9–19, 143–153, 186–194 and 216–223) would adopt. The sequence of α-NGF is more closely related to that of trypsinogen (40.9% identity) than other serine proteinase zymogens with known structures; in trypsinogen, the activation domain (residues 10–19, 142–152, 184–193 and 216–223) is disordered [38]. In the crystal structure of 7S NGF, half of the activation domain of α-NGF (loops 6 and 7) is well-defined and makes extensive contacts with β-NGF, whereas the other half (the N terminus and loop 4, residues A9–A25 and A140–A156) is disordered. Some electron density is visible for the mainchain of CysA157, but there is no density for the CysA157–CysA22 disulphide.

In α-NGF, the disordered loop 4 is cleaved, such that the C-terminal chain starts with TyrA151 [25,26]. This loop is sterically hindered from adopting the same conformation as the equivalent loop in γ-NGF — if it did it would clash with β-NGF. There is, however, some density on the side of the β-NGF dimer, which almost certainly comes from one or two residues in the middle of loop 4 (probably IleA147; Figure 6).

Loops 1 and 8 have conformations unique to α-NGF and interact with γ-NGF. The sidechains of TyrA34 (from the first β strand) and PheA36 (from loop 1) pack against hydrophobic residues from γ-NGF (LeuG95k and IleG173). Loop 8, which is largely disordered, has been pulled sideways (relative to its position in γ-NGF) to provide a zinc-binding residue, GluA75, at the α–γ interface. (The second zinc ligand from α-NGF is HisA82, from the edge strand of the first β sheet.)

Kallikrein loops recognise the C terminus of β-NGF at the β–γ interface

In 7S NGF, the C-terminal arginine residue (B118) of the mature β-NGF is bound in the active site of γ-NGF, probably as a cleaved product. In the refined 7S NGF structure, the distance from the hydroxyl of the active-site serine residue (G195) to the C-terminal carbon of ArgB118 is some 2.7 Å, which is similar to the distance observed for tetrapeptide products bound to *Streptomyces griseus* Protease A [39]. The limited resolution of our

Figure 5

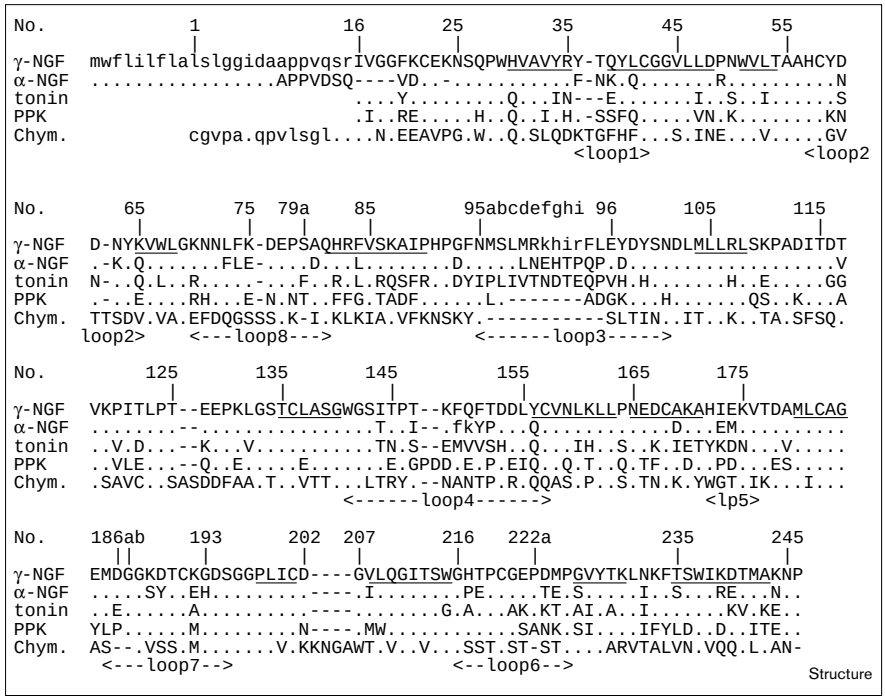

Alignment of γ-NGF, α-NGF and related serine proteinase sequences. The sequences of γ-NGF, α-NGF, rat tonin and PPK are shown aligned with the sequence of bovine chymotrypsinogen. β strands and α helices in γ-NGF are underlined. The positions of eight loops discussed in the text are indicated underneath the alignment, loop 3 is also known as the 'kallikrein loop' and loop 4 as the 'autolysis loop'. The mature sequences of α-NGF and γ-NGF are shown in upper case, with amino acids present only in precursor forms shown in lower case. A dot '.' indicates identity with the sequence of γ-NGF, whereas a '–' indicates a deletion relative to the other serine proteinases.

structure, however, means we cannot rule out the possibility of a covalent bond between the sidechain SerG195 and the C terminus of β-NGF (i.e. an acyl enzyme intermediate).

Blaber *et al.* [40] compared the kinetic constants of γ-NGF, PPK, EGF-BP and bovine pancreatic trypsin for several tripeptide *p*-nitroanilide substrates and found that γ-NGF exhibits the highest affinity (lowest K_m) for most of the substrates examined. This may be partially due to LysG192 in γ-NGF, the sidechain of which packs against PheG149 in the variable autocatalytic loop, and its terminal nitrogen atom makes two hydrogen bonds to the mainchain carbonyls of ThrB117 and LysB74 from β-NGF.

γ-NGF exhibits a pronounced preference for substrates with an arginine rather than a lysine at the P1 position [40] (the P1 position is the first residue on the N-terminal side of the scissile peptide bond). The guanidinium moiety of ArgB118 makes four hydrogen bonds to γ-NGF — two of these are to AspG189, one is to the sidechain hydroxyl of ThrG190 and the fourth is to the carbonyl oxygen of HisG217. The C-terminal arginine of β-NGF is found in the S1 substrate specificity pocket of γ-NGF, explaining why the removal of this arginine residue prevents γ-NGF from associating with β-NGF [41]. The position of ArgB118 is similar to that observed for the P1 arginine in the hirustatin inhibitor–PPK complex [42]. Residues from loops 6 (G215–G224) and 7 (G185–G194) provide most of the residues that constitute the binding pocket for the P1 arginine.

Blaber *et al.* [40] showed that γ-NGF has a marked preference for peptides with a leucine or phenylalanine rather than a threonine residue at the P2 position. The sidechain of ThrB117 of β-NGF (the P2 residue) occupies a broad shallow open pocket between TyrG99 and HisG57, with PheG94 at the back of the pocket. Modelling studies suggest that a leucine would occupy this pocket quite snugly, whereas the substitution of a phenylalanine for ThrB117 would entail some slight movement either of the mainchain of B117 or of the sidechains lining the pocket. The same residues line the S2 pocket in the BPTI–PPK complex (His57, Phe94 and Tyr99), but the positions of PheG94 and TyrG99 are slightly different in γ-NGF. In particular, the sidechain of TyrG99 is rotated inwards to slightly reduce the size of the pocket, possibly as a consequence of packing against TyrG97 and LeuG95c from more distal regions of the kallikrein loop. The P3 position AlaB116 of β-NGF occupies a small cavity between GluG174, TyrG99, TrpG215 and the mainchain of GlyG216, explaining the preference for alanine over glutamate at this position [40].

The kallikrein loop (G94–G100) is involved in extensive interactions with the β-NGF dimer (Figures 3 and 4). The interaction between the β and γ subunits involves an induced fit, which partially orders the kallikrein loop of γ-NGF and the C terminus of β-NGF.

Figure 6

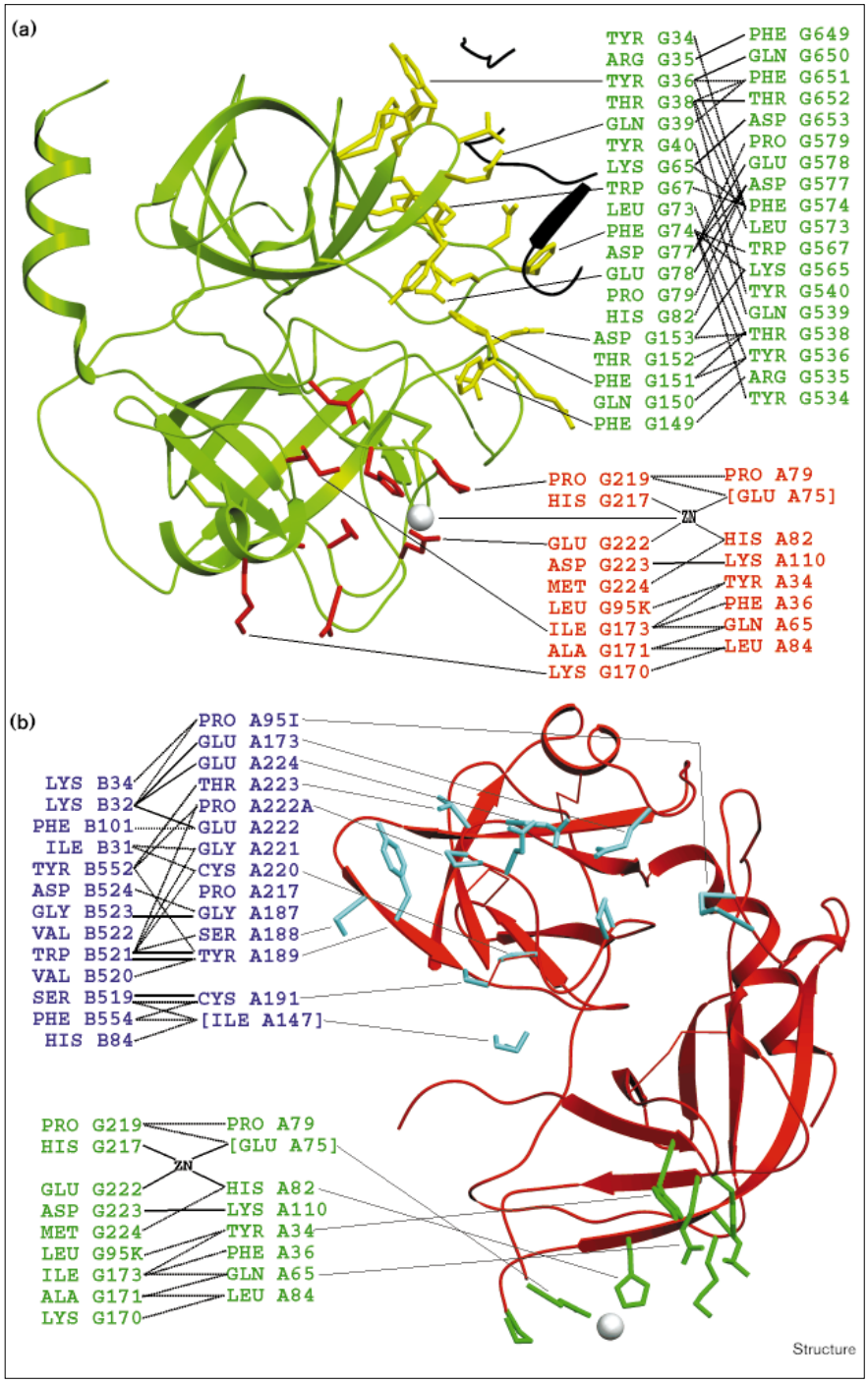

Intermolecular contact residues from α-NGF and γ-NGF subunits. **(a)** The γ-NGF subunit (γ1) from the 7S NGF complex is shown in green, the view is looking down the twofold axis of the complex, and some of the backbone of the twofold related γ2, γ-NGF, subunit is shown in black (namely residues G534–G540, G573–G579 and G649–G653). Sidechains of residues on the γ1, γ-NGF, subunit that interact with the γ2 subunit about the twofold of the complex are shown in yellow. Sidechains of residues that interact with the α1, α-NGF, subunit are shown in red; also shown is the zinc ion (off-white sphere) which mediates the contact between the α1 and γ1 subunits. Contacts between the γ1 and γ2 subunits (in green lettering) and between the γ1 and α1 subunits (red lettering) are indicated as for Figure 3. Residues on the γ1 subunit that contact β-NGF have been omitted from this figure for clarity but are detailed in Figure 3. **(b)** The α1, α-NGF, structure showing residues in light blue (labelled at the top of figure) that interact with the β-NGF dimer. At the bottom of the figure, in green, are residues that interact with the γ1 subunit. The zinc ion is also shown as an off-white sphere. The assignment of IleA147 is tentative, because there is no density for the rest of the autolysis loop.

Both charged and hydrophobic residues are involved in α–β interaction

The acidic α-NGF subunit recognizes a large fairly flat surface comprising residues from both protomers of the basic β-NGF dimer. Residues of α-NGF involved in this interface are largely contributed by loops 6 and 7 (Figure 6) and include the CysA191–CysA220 disulphide bond that links these two loops. This disulphide is part of a hydrophobic patch on the surface of α-NGF (TyrA189, CysA191, CysA220, GlyA221, ProA222a and ProA217) which packs against a complimentary hydrophobic patch on β-NGF (TrpB521, TyrB552, PheB554, PheB101, IleB31, PheB86 and PheB101) which includes residues from both β1 and β2 subunits (Figures 3 and 6). Close to

Figure 7

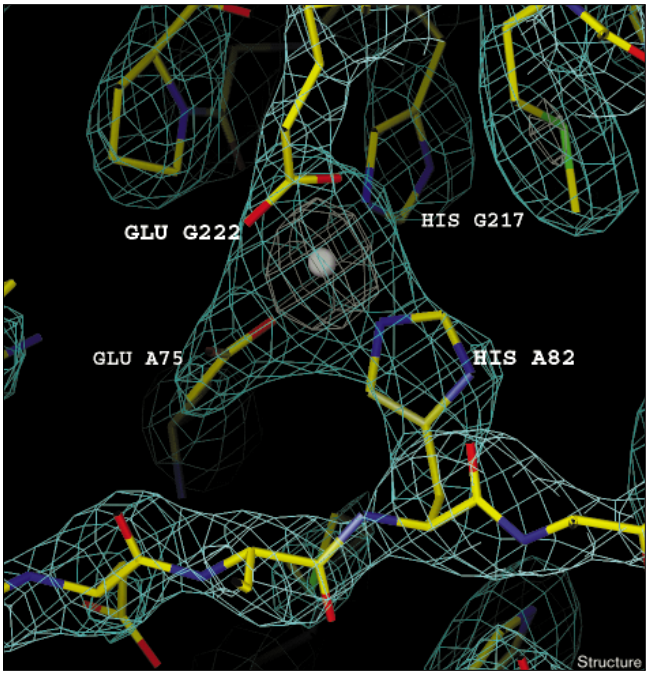

Electron density surrounding the zinc ion (off-white sphere) bound between the α1 and γ1 subunits. The final $2F_o–F_c$ map is shown contoured at 1.5σ (cyan) and 6σ (off-white).

one edge of the α–β interface is an antiparallel β sheet formed between residues GlyA187–CysA191 of α-NGF and GlyB523–SerB519 of β-NGF. A charge–charge interaction on the opposite edge of the interface involves three acidic residues from α-NGF (GluA222, GluA224 and GluA173) that cluster around LysB532 (Figures 3 and 6).

LysB32 is known to play a key role in the interaction of β-NGF with p75NTR, as mutation of LysB32 and LysB34 or LysB95 dramatically reduces binding to p75NTR with the same mutations having only minor effects on the β-NGF–TrkA interaction [43]. The TrkA–binding site of NGF is quite extensive [7,44], and is at least partially occluded by the α subunit. Because residues GluA222 and GluA224 from α-NGF interact with LysB32 of β-NGF, it seems likely that α-NGF will inhibit binding of β-NGF to p75NTR and possibly to TrkA. Peptides derived from loops 6 and 7 of α-NGF (A217–A224 and A187–A192) linked by the CysA191–CysA220 disulphide bond may provide a starting point for the design of peptide inhibitors that block binding of NGF to its receptors.

The two zinc-binding sites are found at the two α–γ interfaces

The α–γ interface is dominated by the presence of a zinc ion (Figures 6 and 7) that has two ligands from γ-NGF — HisG217 and GluG222 — and two from α-NGF — HisA82 and GluA75. The zinc ions are well-ordered with four ligand atoms within 2.4 Å: HisG217 NE2 (2.15 Å), Glu222 OE1 (2.14 Å), HisA82 NE2 (1.84 Å) and GluA75 OE1 (1.85 Å). Additional hydrophobic contacts at the α–γ interface involve TyrA34, PheA36 and LeuA84 packing against LeuG95k, IleG173 and AlaG171; MetG224 is also buried in the interface (Figure 6). The γ-NGF residues at this interface are contributed by loops 5 and 6 with one residue from loop 3 (Figure 6), whereas α-NGF residues come from a β strand (HisA82 and LeuA84), the interdomain connecting peptide (LysA110) and loops 1 and 8 (Figure 6). The binding of the zinc at the α–γ interface is consistent with the observation that zinc enhances the stability of the 7S complex but has no significant effect on the stability of the α–β or β–γ complexes [11,13].

Table 2

Total accessible surface area (Å²) buried in interactions between pairs of subunits.

	β1β2*	γ1	γ2
α1	2373	1667	0
α2	1925	0	1625
γ1	2337	–	2652
γ2	2552	2652	–

*Note the β NGF dimer is treated as a single 'subunit' (the area buried between β1 and β2 is 3033 Å²). Buried areas were calculated in GRASP [57].

An unexpectedly large area is buried between γ1 and γ2 subunits

The area buried between the γ1 and γ2 subunits is the largest in the complex (except that between the β1 and β2 subunits; Table 2). The residues involved in this interaction come primarily from loops 1, 4 and 8 (Figures 6). The twofold axis of the complex passes in between AspG77 and AspG577. The sidechain of AspG77 (AspG577) makes a hydrogen bond to the mainchain amide functions of GluG578 (GluG78). The substitution of three residues in loop 1 of γ-NGF does not affect the ability of γ-NGF to form 7S NGF [45]. Furthermore, although these mutations are close to the γ–γ interface, modelling studies have shown that they are readily accommodated in the 7S structure. The large interface between the two γ subunits (Table 2) is unexpected as in solution γ-NGF is monomeric [11].

Biological implications

Nerve growth factor (NGF) is a differentiation and neuronal survival factor that is under investigation as a potential treatment of specific neurodegenerative diseases. NGF signals through two cell-surface receptors, TrkA and p75NTR, and such signalling can promote cell survival or conversely can lead to apoptosis [3,46]. For many years the primary source of biologically active NGF has

been the mouse submaxilliary gland, where NGF is found in the form of a high molecular weight complex, 7S NGF.

The crystal structure of murine 7S NGF shows how two closely related serine proteinase subunits (α-NGF and γ-NGF) have evolved to recognize the β-NGF dimer. The γ subunit of 7S NGF has acquired the ability to remain bound to the C terminus of β-NGF not only by evolving unique loops that recognize the β-NGF dimer, but also by acquiring a large 'dimeric' interface between the two γ-NGF subunits. This dimeric interface between the γ-NGF subunits is about the same twofold axis that exists within the β-NGF dimer. The α subunit of 7S NGF has evolved from an inactive 'zymogen-like' conformation to recognize β-NGF. The α and γ subunits of 7S NGF are thus not interchangeable — although their sequences are closely related, they have only a 60.6% sequence identity in the eight variable loop regions which make nearly all intersubunit contacts (compared with a 93.9% identity for the remaining residues).

The dimer of the active β-NGF subunits is largely buried in 7S NGF, explaining the lack of neurotrophic activity of the complex. The α-NGF subunit buries residues of the β-NGF dimer, which have been implicated in interactions with both the p75NTR and TrkA receptors. Two loops linked by a disulphide bond provide the majority of the residues from α-NGF that interact with β-NGF and the structure of these two loops could be used as a starting point to design peptides which inhibit the binding of NGF to its receptors.

Materials and methods

Protein crystallization and data collection

We have previously reported the crystallization of two crystal forms of 7S NGF [31], and that the orthorhombic crystal A form ($P2_12_12_1$, a = 95.68 Å, b = 96.59 Å, c = 147.00 Å) diffracts to 2.8 Å. Reprocessing of the original data collected from a single A form crystal at the EMBL outstation at DESY (Hamburg), however, revealed that the diffraction data were very anisotropic and that, although diffraction data did extend to 2.8 Å in the best directions, in other directions the data extended to about 3.5 Å. This dataset was originally processed to 3.3 Å, but reprocessing to 3.1 Å with MOSFLM [47] gave an R_{sym} of 6.5% (Table 3), and this is the only data that has been used for structure determination and refinement.

Optimization of parameters for molecular replacement

A model structure was made by placing two tonin molecules ([29]; PDB code 1TON) next to a β-NGF dimer and then using the twofold axis of the dimer to generate two more tonin subunits giving a model '7S' structure with an internal twofold axis. This model structure was placed in a $P2_12_12_1$ cell with dimensions the same as those of the real cell and structure factors were calculated with programs from the CCP4 suite [48]. The test dataset from this model structure was used to optimize parameters for the self- and cross-rotation functions (both of which were calculated with the program ROTING from the Amore package [49] as implemented on a VAX 11/750 by Huub Driessen).

Self-rotation function

The self-rotation function (Figure 1) clearly showed the presence of a noncrystallographic twofold axis at θ = 72.5°, φ = 82°, χ = 180°. The self-rotation function was calculated with the program ROTING using normalized structure factors (8–3.5 Å), a Patterson search radius of 6–35 Å and l's > 9 (where l is the order of the spherical bessel functions – the omission of small l's is somewhat equivalent to omitting low resolution data in the calculation of the Patterson functions [50]).

Table 3

Crystallographic analysis.

Diffraction data*	
Resolution (Å)	20–3.1 (3.18–3.10)
Unique reflections	24,209
Redundancy	2.5 (2.3)
Completeness	96.0 (92.5)
R_{sym}	6.5 (42.7)
Refinement statistics	
Resolution (Å)	8.0–3.15
No. reflections	21,857
No. protein atoms	8475
No. of Zn^{2+} ions	2
No. NAG atoms	84
Overall anisotropic B factors (scaling F_{obs}–F_{calc})	
B_{11}	−43.24
B_{22}	−0.47
B_{33}	−0.06
R factor (%)	24.6
R_{free} (%)	28.2
Average B factor (Å^2)	40.9
Rmsd bond length (Å)	0.008
Rmsd bond angles (°)	1.75

*Numbers in parentheses refer to data in highest resolution shell.

Cross-rotation functions

A β-NGF search dimer [4] was placed in a P1 cell of dimension 85 × 85 × 85 Å (α = β = γ = 90°) with the internal twofold axis of the dimer aligned parallel to the z axis. It was expected that the twofold axis of the β-NGF dimer would align with the noncrystallographic twofold axis, and a peak was therefore expected in the β-NGF cross-rotation function with Eulerian angles α = 82, β = 72.5 and no restriction for γ. The highest peak in the β-NGF cross-rotation function (α = 83, β = 73, γ = 78) had the expected values of α and β and was therefore clearly the solution (the cross-rotation function was calculated using normalized structure factor amplitudes between 8 and 3.3 Å and a Patterson search radius of 8–29 Å).

The search molecule used to locate the γ-NGF and α-NGF subunits was porcine pancreatic kallikrein (PPK [27]; PDB code 2PKA, first molecule of two molecules in asymmetric unit). The percentage sequence identity of PPK with γ-NGF is 61.6% and that with α-NGF is 56.5%. The kallikrein search molecule was placed in an orthogonal P1 cell of dimension 75 × 75 × 75 Å (α = β = γ = 90°). Cross-rotation functions were searched for pairs of peaks related by the noncrystallographic twofold (with a program cross_chk modified by BB from a program of G Oliva, personal communication). The two highest peaks in the cross-rotation function were related by the noncrystallographic twofold axis and were later found to correspond to the two γ-NGF molecules (cross-rotation function calculated using normalized structure factor amplitudes between 8.0–3.5 Å and Patterson search radii of 4.0–35.0 Å). One of the α-NGF molecules showed up quite well in the cross-rotation function (α1) as the fourth highest peak, whereas the second α-NGF molecule (α2) was the 15th highest peak in the cross-rotation function.

Translation functions

Crystallographic and noncrystallographic translation functions calculated with the CCP4 program TFFC [51] clearly showed the positions of the five subunits in the asymmetric unit (Table 4). Note that the signal for the α2 subunit was in the noise for the crystallographic translation

Table 4

Translation functions.

	Crystallographic				Non-crystallographic*			
Molecule	x	y	z	Height (noise)†	x	y	z	Height (noise)†
β1β2	0.04	0.46	0.36	11.9 (6.1)				
γ1	0.07	0.09	0.14	11.5 (6.1)	0.57	0.59	0.64	17.5 (5.5)
γ2	0.15	0.00	0.38	9.4 (6.3)	0.15	0.00	0.38	16.6 (6.4)
α1	0.31	0.44	0.20	6.7 (5.9)	0.81	0.44	0.20	11.3 (6.6)
α2	0.05	0.26	0.09	4.4 (5.3)	0.05	0.26	0.59	9.9 (6.4)

*Position of β-NGF dimer defined. †The peak height is in rms units. The number in parentheses indicates the height of the second highest peak. The solution was always the highest peak, except for the crystallographic translation function for molecule α2, where it was the 25th highest peak (here the height of the highest peak is indicated in parentheses).

function but was clearly above the noise for the noncrystallographic translation function. Other orientations tried for the α1 and α2 subunits in the translation function did not produce peaks above noise.

Refinement and density modification

Initial rigid-body refinement was carried out with RESTRAIN [52]. $2F_o–F_c$ maps were then calculated and a single pass was made through the entire structure. Examination of the maps showed that the molecular replacement solution was correct, but also showed that the data were very anisotropic (the maps were streaky). The inclusion of an anisotropic scaling step in the refinement decreased the R factor from 46.9 to 43.9% and increased the correlation coefficient from 0.53 to 0.62 (on all data 8.0–3.3 Å). At this stage the original dataset was reprocessed with MOSFLM [47], which confirmed that the anisotropy was an inherent feature of the dataset and was not due to crystal decay.

The structure was then refined with X-PLOR [33], alternating with cycles of manual rebuilding on the computer graphics with O [53]. Overall anisotropic temperature factors, which were used to scale F_{obs} to F_{calc}, were re-calculated in each round of the refinement and these typically decreased both the R factor and R_{free} by 4%. After nine cycles of refinement with X-PLOR and eight rebuilds with O, the final model, which contains 1089 amino acid residues, six *N*-acetyl glucosamine (NAG) residues and two zinc ions, has an R factor of 24.6% (R_{free} of 28.2%) and reasonable geometry (for a structure at this resolution – as assessed with PROCHECK [54]). Note the α2 subunit appears more mobile (mainchain <B> = 45.6 Å^2, sidechain <B> = 53.6 Å^2) than the other subunits (mainchain <B> = 35.6 Å^2, sidechain <B> = 42.8 Å^2). Some more details of the refinement procedure are given below.

The first four rebuilds were carried out largely into maps which had been averaged around the noncrystallographic twofold with RAVE [32], and only one half of the structure was rebuilt. In the second and third cycles of refinement with X-PLOR strict noncrystallographic symmetry (NCS) constraints were applied. The 2.5% of the reflections (612 reflections between 20.0–3.1 Å) flagged in the R_{free} dataset before the start of the refinement procedure were selected in thin resolution shells as suggested by Kleywegt and Jones [55] to avoid the possibility of bias in the R_{free} due to NCS. In each round of refinement, the structure was rebuilt from coordinates which had been subject to conventional positional refinement as simulated annealing or torsion angle refinement protocols invariably resulted in an increase in the R_{free}. Group temperature factors were refined (one for mainchain atoms, one for sidechain atoms) in X-PLOR. The final five cycles of refinement with X-PLOR and four rebuilds with O were performed without NCS constraints/restraints or averaging.

Accession numbers

The coordinates for the 7S NGF structure have been deposited with the Protein Data Bank with the accession code 1SGF.

Acknowledgements

We thank Huub Driessen, Glaucius Oliva and Ian Tickle for help with computing, Keith Wilson and Zbigniew Dauter for assistance with data collection, Steve Wood for advice in the early stages of this project and Ralph Bradshaw for useful discussions.

References

1. Angeletti, R.H. & Bradshaw, R.A. (1971). Nerve growth factor from mouse submaxillary gland: amino acid sequence. *Proc. Natl. Acad. Sci. USA* **68**, 2417–2420.
2. Barde, Y.-A. (1994). Neurotrophic factors: an evolutionary perspective. *J. Neurobiol.* **25**, 1329–1333.
3. Kaplan, D.R. & Miller, F.D. (1997). Signal transduction by the neurotrophin receptors. *Curr. Opin. Cell Biol.* **9**, 213–221.
4. McDonald, N.Q., Lapatto, R., Murray-Rust, J., Gunning, J., Wlodawer, A. & Blundell, T.L. (1991). New protein fold revealed by a 2.3 Å resolution structure of nerve growth factor. *Nature* **354**, 411–414.
5. Murray-Rust, J., *et al*., & Bradshaw, R.A. (1993). Topological similarities in TGF-β2, PDGF-BB and NGF define a superfamily of polypeptide growth factors. *Structure* **1**, 153–159.
6. Bradshaw, R.A., Murray-Rust, J., Ibáñez, C.F., McDonald, N.Q., Lapatto, R. & Blundell, T.L. (1994). Nerve growth factor. Structure/function relationships. *Protein Sci.* **3**, 1901–1913.
7. Ibáñez, C.F. (1995). Neurotrophic factors: from structure function studies to designing effective therapeutics. *Trends Biotech.* **13**, 217–227
8. Levi-Montalcini, R. (1987). The nerve growth factor 35 years later. *Science* **237**, 1154–1162.
9. Varon, S., Nomura, J. & Shooter, E.M. (1967). Subunit structure of a high-molecular-weight form of the nerve growth factor from mouse submaxillary gland. *Proc. Natl. Acad. Sci. USA* **57**, 1782–1789.
10. Varon, S., Nomura, J. & Shooter, E.M. (1968). Reversible dissociation of the mouse nerve growth factor protein into different subunits. *Biochemistry* **7**, 1296–1303.
11. Silverman, R.E. & Bradshaw, R.A. (1982). Nerve growth factor: subunit interactions in the mouse submaxillary gland 7S complex. *J. Neurosci. Res.* **8**, 127–136.
12. Pattison, S.E. & Dunn, M.F. (1975). On the relationship of zinc ion to the structure and function of the 7S nerve growth factor protein. *Biochemistry* **14**, 2733–2739.
13. Bothwell, M.A. & Shooter, E.M. (1978). Thermodynamics of interaction of the subunits of 7S nerve growth factor – the mechanism of activation of the esteropeptidase activity by chelators. *J. Biol. Chem.* **253**, 8458–8464.
14. Palmer, T.E. & Neet, K.E. (1980). Subunit interactions in 7S nerve growth factor. γ-Esterase activity as a probe of the dissociation of the 7S oligomer by salt and EDTA. *J. Biol. Chem.* **255**, 5170–5176.
15. Palmer, T.E. & Neet, K.E. (1980). Subunit interactions in 7S nerve growth factor: Sedimentation analysis of the dissociation of the 7S oligomer promoted by salt and ethylenediaminetetracetate. *Arch. Biochem. Biophys.* **205**, 412–421.

16. Rao, A.G. & Neet, K.E. (1984). Subunit interactions of 7S nerve growth factor: γ-Esterase activity, rates and conformational changes during reassociation. *J. Biol. Chem.*, **259**, 73–79.
17. Harris-Warwick, R.M., Bothwell, M.A. & Shooter, E.M. (1980). Subunit interactions inhibit the binding of β nerve growth factor to receptors on embryonic chick sensory neurons. *J. Biol. Chem.* **255**, 11284–11289.
18. Stach, R.W. & Shooter, E.M. (1980). Cross-linked 7S nerve growth factor is biologically inactive. *J. Neurochem.* **34**, 1499–1505
19. Woodruff, N.R. & Neet, K.E. (1986). Inhibition of β nerve growth factor binding to PC12 cells by α nerve growth factor and γ nerve growth factor. *Biochemistry* **25**, 7967–7974.
20. Thomas, K.A., Baglan, N.C. & Bradshaw, R.A. (1981). The amino acid sequence of the γ-subunit of mouse submaxillary gland 7S nerve growth factor. *J. Biol. Chem.* **256**, 9156–9166.
21. Ullrich, A., Gray, A., Wood, W.I., Hayflick, J. & Seeburg, P.H. (1984). Isolation of a cDNA clone coding for the γ-subunit of mouse nerve growth factor using a high-stringency selection procedure. *DNA* **3**, 387–392.
22. Isackson, P.J., Ullrich, A. & Bradshaw, R.A. (1984). Mouse 7S nerve growth factor: complete sequence of a cDNA coding for the α-subunit precursor and its relationship to serine proteases. *Biochemistry* **23**, 5997–6002
23. Edwards, R.H., Selby, M.J., Garcia, P.O. & Rutter, R.J. (1988). Processing of the native nerve growth factor precursor to form biologically active nerve growth factor. *J. Biol. Chem.* **263**, 6810–6815.
24. Jongstra-Bilen, J., Coblentz, L. & Shooter, E.M. (1989). The *in vitro* processing of the NGF precursors by the γ-subunit of the 7S NGF complex. *Brain Res. Mol. Brain Res.* **5**, 159–169.
25. Isackson, P.J. & Bradshaw, R.A. (1984). The α-subunit of mouse 7S nerve growth factor is an inactive serine protease. *J. Biol. Chem.* **259**, 5380–5383.
26. Ronne, H., Anundi, H., Rask, L. & Peterson, P.A. (1984). 7S nerve growth factor α and γ subunits are closely related subunits. *Biochemistry* **23**, 1229–1234.
27. Bode, W., Chen, Z., Bartels, K., Kutzbach, C., Schmidt-Kastner, G. & Bartunik, H. (1983). Refined 2 Å X-ray crystal structure of porcine pancreatic kallikrein A, a specific trypsin-like serine protease. *J. Mol. Biol.* **164**, 237–282.
28. Chen, Z. & Bode, W. (1983). Refined 2.5 Å X-ray crystal structure of the complex formed by porcine kallikrein A and the bovine pancreatic trypsin inhibitor. *J. Mol. Biol.* **164**, 283–311.
29. Fujinaga, M. & James, M.N.G. (1987). Rat submaxillary gland serine protease tonin: structure and solution refinement at 1.8 Å resolution. *J. Mol. Biol.* **195**, 373–396.
30. Bax, B., Blaber, M., Ferguson, G., Sternberg, M.J.E. & Walls, P.H. (1993). Prediction of the three-dimensional structures of the nerve growth factor and epidermal growth factor binding proteins (kallikreins) and an hypothetical structure of the high molecular weight complex of epidermal growth factor with its binding protein. *Protein Sci.* **2**, 1229–1241.
31. McDonald, N.Q. & Blundell, T.L. (1991). Crystallization and characterization of the high molecular weight form of nerve growth factor (7S NGF). *J. Mol. Biol.* **219**, 595–601.
32. Kleywegt, G.J. & Jones, T.A. (1994). Halloween ... masks and bones. In *From First map to Final Model.* (Bailey, S., Hubbard, R., & Waller, D., eds), pp. 59–65, SERC Daresbury Laboratory, Daresbury, UK.
33. Brünger, A.T. (1992). *X-PLOR Version 3.1: A System for X-ray Crystallography and NMR.* Yale University Press, New Haven & London.
34. Holland, D.R., Cousens, L.S., Meng, W. & Matthews, B.W. (1994). Nerve growth factor in different crystal forms displays structural flexibility and reveals zinc binding sites. *J. Mol. Biol.* **239**, 385–400.
35. Mobley, W.C., Schenker, A. & Shooter, E.M. (1976). Characterization and isolation of proteolytically modified nerve growth factor. *Biochemistry* **15**, 5543–5551.
36. Thomas, K.A., Silverman, R.E., Jeng, I., Baglan, N.C. & Bradshaw, R.A. (1981). Electrophoretic heterogeneity and polypeptide chain structure of the γ-subunit of mouse submaxillary gland 7S nerve growth factor. *J. Biol. Chem.* **256**, 9147–9155.
37. Burton, L.E. & Shooter, E.M. (1981). The molecular basis of the heterogeneity of the γ subunit of 7S nerve growth factor. *J. Biol. Chem.* **256**, 11011–11017.
38. Walter, J., Steigemann, W., Singh, T.P., Bartunik, H., Bode, W. & Huber, R. (1982). On the disordered activation domain in trypsinogen: chemical labelling and low-temperature crystallography. *Acta Cryst. B* **38**, 1462–1472.
39. James, M.N.G., Sielecki, A.R., Brayer, G.D. & Delbaerre, L.T.J. (1980). Structures of product and inhibitor complexes of *Streptomyces griseus* protease A at 1.8 Å resolution. *J. Mol. Biol.* **144**, 43–88.
40. Blaber, M., Isackson, P.J., Marsters, J.C. Jr., Burnier, J.P. & Bradshaw, R.A. (1989). Substrate specificities of growth factor associated glandular kallikreins of the mouse submandibular gland. *Biochemistry* **28**, 7813–7819.
41. Moore, J.B., Mobley, W.C. & Shooter, E.M. (1974). Proteolytic modification of the β nerve growth factor protein. *Biochemistry* **13**, 833–840.
42. Mittl, P.R.E., *et al.*, & Grütter, G.G. (1997). A new structural class of serine protease inhibitors revealed by the structure of the hirustatin–kallikrein complex. *Structure* **5**, 253–264.
43. Ibáñez, C.F., Ebendal, T., Barbany, G., Murray-Rust, J., Blundell, T.L. & Persson, H. (1992). Disruption of the low affinity receptor-binding site in NGF allows neuronal survival and differentiation by binding to the *trk* gene product. *Cell* **69**, 329–341.
44. Ibáñez, C.F., Ilag, L.L., Murray-Rust, J., & Persson, H. (1993). Chimeric molecules with multiple neurotrophic activities reveal structural elements determining the specificities of NGF and BDNF. *EMBO J.* **10**, 2105–2110.
45. Blaber, M., Isackson, P.J., Holden, H.M. & Bradshaw, R.A. (1993). Synthetic chimeras of mouse growth factor associated glandular kallikreins. II. Growth factor binding properties. *Protein Sci.* **2**, 1220–1228
46. Casaccia-Bonnefil, P., Carter, B.D., Dobrowsky, R.T. & Chao, M.V. (1996). Death of oligodendrocytes mediated by the interaction of nerve growth factor with its receptor p75. *Nature* **383**, 716–719.
47. Leslie, A.G.W., Brick, P. & Wonacott, A.T. (1986). *An improved package for the measurement of oscillation photographs. Daresbury Laboratory Information Quarterly for Protein Crystallography, Vol 18.* pp. 33–39, SERC Daresbury Laboratory, Warrington, UK.
48. CCP4 (1994). The CCP4 Suite: programs for protein crystallography. *Acta Cryst. D* **50**, 760–763.
49. Navaza, J (1994). AMoRe: an automated package for molecular replacement. *Acta Cryst. A* **50**, 157–163
50. Navaza, J (1987). On the fast rotation function. *Acta Cryst. A* **43**, 645–653
51. Tickle, I. (1985). Review of space group general translation functions that make use of known structure information and can be expanded as fourier series. In *Molecular Replacement.* (Machin, P.A., ed.), pp. 22–26, SERC Daresbury Laboratory, Warrington, UK.
52. Driessen, H.P.C., Haneef, M.I.J., Harris, G.W., Howlin, B., Khan, G. & Moss, D.S. (1989). RESTRAIN: restrained structure-factor least-squares refinement program for macromolecular refinement. *J. Appl. Cryst.* **22**, 510–516.
53. Jones, T.A., Zou, J.–Y., Cowan, S.W. & Kjeldgaard, M. (1991). Improved methods for building protein models in electron density maps and the location of errors in these models. *Acta Cryst A* **47**, 110–119.
54. Laskowski, R.A., MacArthur, M.W., Moss, D.S. & Thornton, J.M. (1993). PROCHECK: a program to check stereochemical quality of protein structures. *J. Appl. Cryst.* **26**, 283–291.
55. Kleywegt, G.J. & Jones, T.A. (1995). Where freedom is given liberties are taken. *Structure* **3**, 535–540.
56. Evans, S.V. (1993). SETOR: hardware lighted three-dimensional solid model representations of macromolecules. *J. Mol. Graphics.* **11**, 134–138.
57. Nichols, A., Sharp, K.A. & Honig, B. (1991). Protein folding and association: insights from the interfacial and thermodynamic properties of hydrocarbons. *Proteins* **11**, 281–296.
58. Kraulis, P.J. (1991). MOLSCRIPT: a program to produce both detailed and schematic plots of protein structures. *J. Appl. Cryst.* **24**, 946–950.